

# Towards Omni-supervised Referring Expression Segmentation

Minglang Huang<sup>1</sup>, Yiyi Zhou<sup>1,2</sup>, Gen Luo<sup>1</sup>, Guannan Jiang<sup>3</sup>, Weilin Zhuang<sup>3</sup>, Xiaoshuai Sun<sup>1,2</sup>

<sup>1</sup>Key Laboratory of Multimedia Trusted Perception and Efficient Computing,  
Ministry of Education of China, Xiamen University, 361005, P.R. China.

<sup>2</sup>Institute of Artificial Intelligence, Xiamen University, 361005, P.R. China.

<sup>3</sup>Intelligent Manufacturing Department, Contemporary Amperex Technology Co. Limited (CATL).

{huangminglang, luogen}@stu.xmu.edu.cn,

{zhouyiyi, xssun}@xmu.edu.cn, {jianggn, ZhuangWL}@catl.com

## Abstract

Referring Expression Segmentation (RES) is an emerging task in computer vision, which segments the target instances in images based on text descriptions. However, its development is plagued by the expensive segmentation labels. To address this issue, we propose a new learning task for RES called *Omni-supervised Referring Expression Segmentation* (Omni-RES), which aims to make full use of unlabeled, fully labeled and weakly labeled data, *e.g.*, referring points or grounding boxes, for efficient RES training. To accomplish this task, we also propose a novel yet strong baseline method for Omni-RES based on the recently popular teacher-student learning, where the weak labels are not directly transformed into supervision signals but used as a yardstick to select and refine high-quality pseudo-masks for teacher-student learning. To validate the proposed Omni-RES method, we apply it to a set of state-of-the-art RES models and conduct extensive experiments on a bunch of RES datasets. The experimental results yield the obvious merits of Omni-RES than the fully-supervised and semi-supervised training schemes. For instance, with only 10% fully labeled data, Omni-RES can help the base model achieve 100% fully supervised performance, and it also outperform the semi-supervised alternative by a large margin, *e.g.*, +14.93% on RefCOCO and +14.95% on RefCOCO+, respectively. More importantly, Omni-RES also enable the use of large-scale vision-languages like Visual Genome to facilitate low-cost RES training, and achieve new SOTA performance of RES, *e.g.*, 80.66 on RefCOCO. Our code is anonymously released at: <https://github.com/nineblu/omni-res>.

## Introduction

Referring Expression Segmentation (RES) (Yu et al. 2016; Luo et al. 2020b,a; Zhu et al. 2022), also called *Referring Image Segmentation* (Jing et al. 2021; Li et al. 2021c; Wang et al. 2021), aims to ground the visual instances via binary segmentation masks according to the given natural language expressions. Compared with conventional segmentation tasks (Long, Shelhamer, and Darrell 2014; He et al. 2017), RES merits in its flexibility and generalization ability, where the segmentation can be flexibly decided by the text descriptions. Thus, it has great potential in a wide range of applications, such as video surveillance, image editing and human-computer interaction. However, its annotation, *i.e.*, segmentation masks, is time-consuming and labor-intensive,

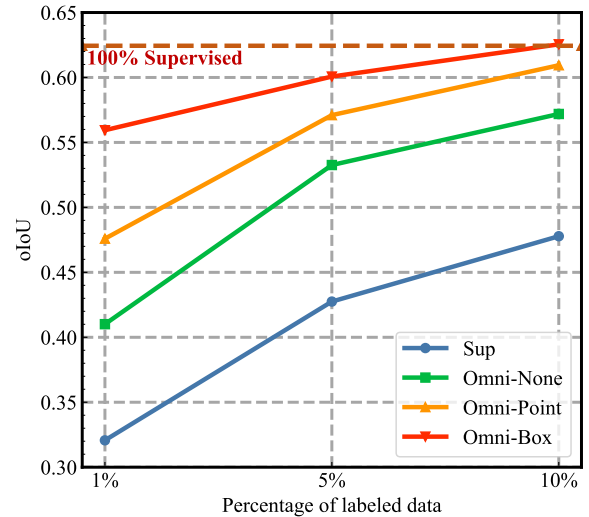


Figure 1: Omni-RES significantly improve the performance of RES with limited mask annotations. With 10% fully labeled data, Omni-RES can help our base model SimRES achieve 100% supervised performance.

which greatly plagues the its development.

However, there exists massive high-quality but weakly-labeled data in vision-language research (Ordonez, Kulka-rni, and Berg 2011; Lin et al. 2014; Krishna et al. 2016; Sharma et al. 2018). For instance, the popular Visual Genome dataset (Krishna et al. 2016) has over 6 millions of grounding boxes, which are also annotated according to the text expression. More recently, these additional data has been exploited to boost the development of referring expression comprehension (REC) (Luo et al. 2022; Zhu et al. 2022), a similar task to RES. But so far, there is still no feasible way for RES to exploit these much cheaper annotations.

Inspired by the recent progress in computer vision (Wang et al. 2022), we propose a new training task for RES towards the effective use of low-cost VL labels, termed *Omni-supervised Referring Expression Segmentation* (Omni-RES). Compared with the semi-supervised or weakly-supervised learning schemes (Strudel, Laptev, and Schmid

2022; Li et al. 2022; Feng et al. 2022), Omni-RES has no strict restrictions on its training data, which can be the unlabeled, fully labeled or weakly labeled ones. In particular, we focus on the exploration of the weak labels of grounding boxes and referring points, which are much cheaper to annotate and easier to obtain from existing datasets. By including these weakly-labeled data, we can achieve much better performance than fully-supervised learning, which is even on par with the fully supervised performance at the same data scale, as shown in Fig. 1.

To accomplish Omni-RES, we further propose a strong baseline method in this paper, of which structure is depicted in Fig. 2. This baseline scheme applies the teacher-student learning (Liu et al. 2021b; Mi et al. 2022) to train the RES models via the self-consistency based objectives with limited label information. In terms of the weak labels, *e.g.*, grounding boxes or points, they are not directly transformed into supervision signals through complex operations, as most existing weakly supervised methods do in other tasks (Ahn and Kwak 2018a; Zhang et al. 2020; Wang et al. 2020a; Sun et al. 2020; Oh, Kim, and Ham 2021). Instead, we use them as yardsticks to select and produce high-quality pseudo-masks predicted by the teacher. The intuition is that the quality of pseudo-labels plays a critical role in teacher-student learning (Liu et al. 2021b; Xu et al. 2021; Li et al. 2021a), which is decisive for the final performance. With the above designs, Omni-RES can well exploit massive unlabeled and low-cost labeled data with limited label information, thereby achieving inexpensive RES training.

To validate Omni-RES, we first propose a base model based on a lightweight REC model (Luo et al. 2022) for quick validations, termed SimRES. Meanwhile, we also examine Omni-RES on two recently proposed RES models, namely LAVT (Yang et al. 2021b) and ReLA (Liu, Ding, and Jiang 2023). Numerous experiments are conducted on three RES benchmarks (Yu et al. 2016; Mao et al. 2015; Nagaraja, Morariu, and Davis 2016). The experimental results show that Omni-RES can achieve +24.59% and +16.24% improvements on average with omni-labels of grounding boxes and points, respectively. Notably, Omni-RES can help SimRES achieve 100% fully supervised performance with only 10% labeled data. Its advantages to the semi-supervised baseline are also distinct, *e.g.*, +14.93% on RefCOCO with 1% labeled data. Meanwhile, Omni-RES also help ReLA achieve new SOTA performance on these benchmarks, *e.g.*, 80.66 on RefCOCO *testA*.

Overall, our contribution is three-fold.

- We introduce a new learning task for RES to address the issue of insufficient label information, termed Omni-RES, which aims to use unlabeled, weakly labeled and fully labeled data for efficient RES training.
- To accomplish Omni-RES, we also propose a strong baseline method with a novel teacher-student learning scheme, where the weak labels are used as a yardstick to select and refine pseudo-masks.
- On three benchmark datasets, Omni-RES can achieve superior performance gains than the fully-supervised and semi-supervised baselines. Notably, with only 10% fully

labeled data, Omni-RES can help the model achieve 100% supervised performance.

## Related Work

### Referring Expression Segmentation

Referring expression segmentation (RES) aims to segment the target object in an image according to a given natural language expression. (Hu, Rohrbach, and Darrell 2016) Early RES works (Liu et al. 2018; Yu et al. 2018) usually follow a two-stage pipeline, and formulate RES as an object-expression matching problem. Recently, one-stage RES models (Liu et al. 2017; Margffoy-Tuay et al. 2018; Li et al. 2018) have attracted increasing attentions recently, where the RES model embeds the text features into a segmentation network, and directly predict the mask of the referent. Inspired by the great success of Transformer, a variety of Transformer-based RES models are proposed recently (Ding et al. 2022; Kim et al. 2022; Li and Sigal 2021; Zhao et al. 2023; Liu, Ding, and Jiang 2023; Liu et al. 2023). VLT (Ding et al. 2022) takes fusion of vision and language as input to transformer encoder-decoder framework, and RESTR (Kim et al. 2022) uses transformer encoders for the two modalities independently. In addition to the design of network structure, some recent advances also investigate the early fusion strategy (Li et al. 2021c; Yang et al. 2021b) and the multi-modal alignment loss (Wang et al. 2021) to boost performance.

### Omni-Supervised Learning

Omni-supervised learning (OSL) aims to combine different forms of annotations, *i.e.*, tag and point, to supervise the model (Radosavovic et al. 2017; Ren et al. 2020; Wang et al. 2022). (Radosavovic et al. 2017) is the first to propose the idea of omni-supervised learning, which uses internet-scale sources of unlabeled data for keypoint detection and object detection. After that, UFO<sup>2</sup> (Ren et al. 2020) considers more forms of annotation inferior to box as weakly labeled annotations for object detection, such as tag, point and scribble. In this method, tag can provides the information of class about the object which is hoped to be detected in the image. Similarly, point and scribble can provide some level of localization information of the object in the image, which facilitates the omni-supervised learning, far better than just using unlabeled data. Recently, Omni-DETR (Wang et al. 2022), based on DETR (Carion et al. 2020), proposes a unified framework to combine different forms of annotations, which maximizes the use of weakly labeled data for object detection, including tags, points without tags, boxes without tags, points with tags and tags with counts. Although OSL has been widely applied in object detection, it still lacks an exploration on segmentation-related task (Long, Shelhamer, and Darrell 2014; Chen et al. 2016; He et al. 2017; Chen et al. 2020; Kirillov et al. 2018; Li, Arnab, and Torr 2018; Luo et al. 2023a,b). In this paper, we commit the first attempt on the segmentation-based task, *i.e.*, RES, which allows for the integration of points and boxes as weakly labeled annotations.

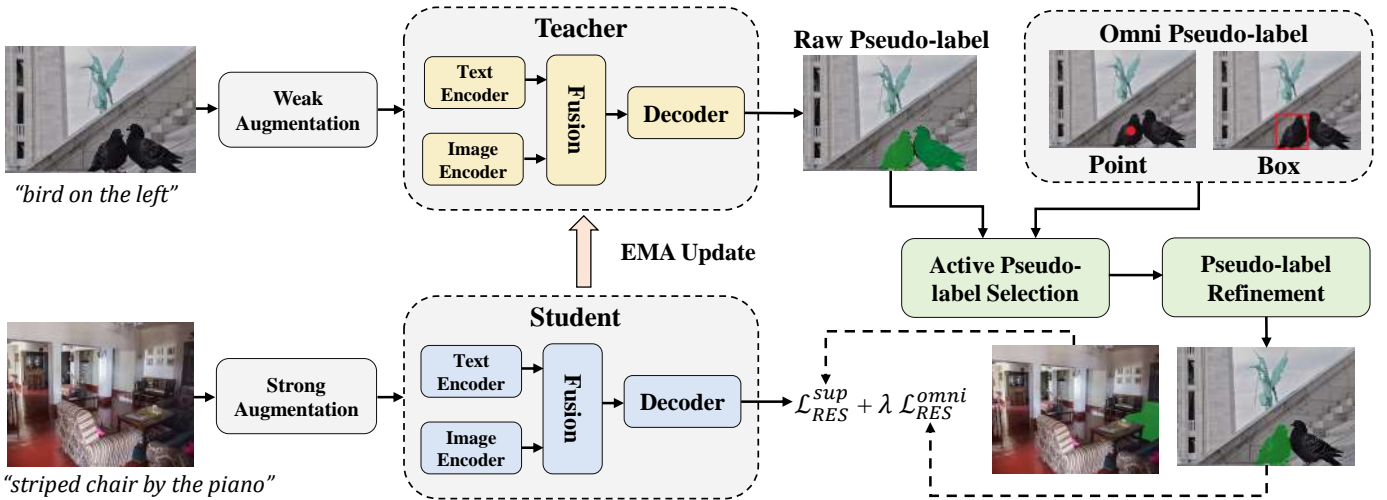


Figure 2: **Overall of the proposed baseline training paradigm for Omni-RES.** This paradigm uses a teacher-student framework, where the Teacher and the Student networks are initialized with the same RES models. During omni-training, the teacher is in charged of producing pseudo segmentation masks for the student with the limited fully label information. The omni-labels, *i.e.*, point or box, are applied to actively refine the raw pseudo-labels, thereby improving the teacher-student learning.

## Method

### Task Definition

Omni-supervised referring expression segmentation (Omni-RES) aims to exploit unlabeled, fully labeled and weakly labeled data to facilitate model training. Given a set of fully labeled data  $D_f = \{(x_i, t_i, y_i^f)\}_{i=1}^N$  and omni-labeled data  $D_o = \{(x_j, t_j, y_j^o)\}_{j=1}^M$ , the objective of omni-supervised RES  $\mathcal{L}$  is formulated as

$$\min \mathcal{L}(\theta; D_f, D_o). \quad (1)$$

Here,  $x$ ,  $t$  and  $y$  denote the input images, texts and labels, respectively.  $N$  and  $M$  are the numbers of fully-labeled and omni-labeled examples.  $\theta$  denotes the model’s parameters.

In particular, the effectiveness of omni-supervised learning is highly dependent on the design of omni-labels  $y_j^o$  (Wang et al. 2022). Omni-labels need to provide useful information for RES, and should be easier to access than the segmentation masks. In this case, we define three types of omni-labels below:

- **None** ( $y^o = \emptyset$ ). It means no annotations in  $D_o$ . In this case, Omni-RES can also be regraded as a semi-supervised learning process in this paper, when  $D_o$  is the unlabeled data.
- **Point** ( $y^o = \{p_j\}_{j=1}^M$ ). The grounding point is defined by the geometric center of the referred object, as shown in Fig.2. Point tag is actually cheap and effortless, but can provide the location prior of the referent, which is critical for RES task.
- **Box** ( $y^o = \{b_j\}_{j=1}^M$ ). It denotes the bounding box of the target object. This type of labeling is slightly more expensive than point, but still much easier than the binary mask of RES. As revealed in (Luo et al. 2020b), grounding box can well help the RES model locate the object and refine the segmentation results.

Compared with existing OSL works (Ren et al. 2020; Wang et al. 2022), we omit other weak labels such as semantic tags, object counts and visual traces (scribbled). To explain, semantic tags are redundant to the text information of RES’s expressions, and object counts are of limited importance to RES. The visual traces and scribbles are potentially helpful to Omni-RES, but their access are relatively difficult than box and points in existing VL datasets.

### Omni-RES

**Overall framework.** To achieve Omni-RES, we propose a strong baseline training paradigm in this paper, of which framework is depicted in Fig. 2. In particular, the optimization objective of Omni-RES is defined by

$$\mathcal{L} = \mathcal{L}_{\text{sup}} + \lambda \mathcal{L}_{\text{omni}}, \quad (2)$$

where  $\mathcal{L}_{\text{sup}}$  and  $\mathcal{L}_{\text{omni}}$  denote the supervised and omni-supervised objective functions, respectively.  $\lambda$  is the hyper-parameter to adjust the weight of  $\mathcal{L}_{\text{omni}}$ . For RES, the supervised objective is defined by

$$\mathcal{L}_{\text{sup}}(\theta; x_i, t_i, y_i^f) = - [y_i^f \log(G(x_i, t_i|\theta)) + (1 - y_i^f) \log(1 - G(x_i, t_i|\theta))], \quad (3)$$

where  $G(x_i, t_i|\theta)$  denotes the binary predictions.

To maximize the benefits of omni-supervised learning, it is essential to design an effective objective  $\mathcal{L}_{\text{omni}}$  for RES. In existing segmentation research (Zhou et al. 2015; Jiang et al. 2022; Wang et al. 2020b; Ahn and Kwak 2018b), these weak labels are often transformed into direct supervisions via *Classification Activation Map* (Zhou et al. 2015) or *Self-supervised Equivariant Attention Mechanism* (Wang et al. 2020b). However, RES examples often contains more sparser label information, *e.g.*, only one target corresponding to the expression. And existing weakly-supervised methods still cannot yield supervision signals with satisfactory

quality for RES (Strudel, Laptev, and Schmid 2022; Li et al. 2022; Feng et al. 2022). In this case, we regard Omni-RES as a teacher-student based pseudo-learning process.

In particular, Omni-RES consists of two networks with the same configurations, namely teacher and student. Similar to semi-supervised methods (Sohn et al. 2020; Liu et al. 2021b; Xu et al. 2021), the teacher is used to predict pseudo-labels for optimizing the student, while the parameters of the student will be used to update the teacher via EMA (Tarvainen and Valpola 2017), as shown in Figure 2.

During teacher-student learning, Omni-labels are leveraged to select and refine the pseudo-labels, thereby significantly improving the effectiveness of teacher-student learning. To this end,  $\mathcal{L}_{\text{omni}}$  is defined by

$$\begin{aligned} \mathcal{L}_{\text{omni}}(\theta; x_j, t_j, y_j^o) = & -[y_j^{o'} \log(G(x_j, t_j|\theta)) \\ & + (1 - y_j^{o'}) \log(1 - G(x_j, t_j|\theta))], \\ \text{where } y_j^{o'} = & r(y_j^o, G_t(x_j, t_j|\theta)). \end{aligned} \quad (4)$$

Here,  $G(\cdot)$  and  $G_t(\cdot)$  denote the student and teacher, respectively, and  $r(\cdot)$  represents the active pseudo-label refinement schemes proposed in this paper, which are based on omni-labels. During training, the teacher’s parameters  $\theta_t$  are updated from the student via EMA (Tarvainen and Valpola 2017), which can be formulated by

$$\theta_t^k \leftarrow \alpha \theta_t^{k-1} + (1 - \alpha) \theta^k, \quad (5)$$

where  $k$  is the training step and  $\alpha$  denotes the keeping rate. To alleviate error accumulation (Liu et al. 2021b), we apply strong data augmentations to the input images of the student and teacher, respectively.

**Active Pseudo-Label Refinement** In teacher-student learning, the quality of pseudo-labels is decisive for the final performance (Liu et al. 2021b; Xu et al. 2021; Li et al. 2021b). For Omni-RES, the problem of low-quality pseudo-labels is much more significant than other tasks, e.g., object detection (Sohn et al. 2020; Liu et al. 2021b; Xu et al. 2021; Tang et al. 2021). At the initial training stage, the model is prone to producing scattered and erroneous pseudo-masks.

To overcome this challenge, we propose *Active Pseudo-Label Refinement* (APLR) to refine and filter pseudo-masks by using omni-labels  $y_i^o$  as visual priors to obtain high-quality pseudo-label  $y_j^{o'}$  for optimizing omni-supervised objective in Eq. 4, which is an essential procedure in the framework of Omni-RES. As depicted in Fig. 2, APLR consists of two steps. The first step is *Active Pseudo-label Selection*, which select the plausible segmented masks filtered with omni-labels from the raw pseudo-labels. The second step is *Pseudo-label Refinement*, which means that after selection, we keep the selected masks and discard the other masks to refine raw pseudo-labels for training.

Specifically, in *Active Pseudo-label Selection*, we propose two selection metrics for the omni-labels of point and box, respectively.

The selection metric for omni-points  $s_p$  is formulated by

$$s_p^j = \mathbb{I}(p_j \cap m_j \neq \emptyset), \quad (6)$$

where  $m_j$  denotes the pseudo-masks predicted by the teacher.  $\mathbb{I} : X \rightarrow \{0, 1\}$  is the indicator function. Eq. 6 means that if the point annotation does not fall in any segmented area of the pseudo-mask, i.e.,  $s_p^j = 0$ , the pseudo-mask is likely to be negative label and will be skipped during training. In practice, we apply the topological method in (Suzuki et al. 1985) to disentangle the multiple predicted segmented areas which are not connected to each other in the pseudo-masks, and then select the plausible segmented areas in which point  $p_j$  falls.

For omni-boxes, the selection metric  $s_b$  is defined by

$$s_b^j = \mathbb{I}\left(\frac{\sum b'_j m_j}{h_b^j \times w_b^j} > \tau\right), \quad (7)$$

where  $h_b^j$  and  $w_b^j$  denote the height and width of box  $b_j$ , and  $\tau$  is the threshold. When the segmented area is zero, i.e.,  $b'_j = 0$  means that the predicted mask is incorrect, so we can directly discard this negative pseudo-label. Similarly, when the predicted area is smaller than the threshold, i.e.,  $s_b = 0$ , the quality of pseudo-mask is poor and can be ignored.

In *Pseudo-label Refinement*, to obtain refined pseudo-labels  $y_j^{o'}$  from raw pseudo-labels, we filter out the predicted masks where  $s^j = 0$  based on the two selection metrics and keep the rest.

With the above filtering schemes, we can greatly improve the quality of pseudo-labels, thereby boosting the performance of Omni-RES.

---

#### Algorithm 1: Pseudo Code of Omni-RES

---

**Input:** Labeled Dataset  $\{\mathcal{X}^0, \mathcal{T}^0, \mathcal{Y}_F^0\}$ , Omni-labeled Dataset  $\{\mathcal{X}^0, \mathcal{T}^0, \mathcal{Y}_O^0\}$ , Maximum Iteration  $K$   
**Output:** Student Model  $M^s$

- 1: **for all**  $i = 1, \dots, K$  **do**
- 2:     **for all**  $(x, t, y_f) \in \{\mathcal{X}^0, \mathcal{T}^0, \mathcal{Y}_F^0\}$  **do**
- 3:         Calculate supervised loss using Student network  $M_{i-1}^t$  by Eq. 3
- 4:     **for all**  $(x, t, y_o) \in \{\mathcal{X}^0, \mathcal{T}^0, \mathcal{Y}_O^0\}$  **do**
- 5:         Output raw pseudo-labels of omni-labeled data using Teacher network  $M_{i-1}^t$
- 6:         Filter raw pseudo-labels into refined pseudo-labels using *Active Pseudo-label Refinement* by Eq. 6 and Eq. 7
- 7:         Calculate omni-supervised loss using refined pseudo-labels by Eq. 4
- 8:     **for all**  $(x, t, y_f) \in \{\mathcal{X}^0, \mathcal{T}^0, \mathcal{Y}_F^0\}$  and  $(x, t, y_o) \in \{\mathcal{X}^0, \mathcal{T}^0, \mathcal{Y}_O^0\}$  **do**
- 9:         Update the parameters of Student  $M_i^s$  by Eq. 2
- 10:         Update the parameters of Teacher  $M_i^t$  by Eq. 5
- 11:     **end for**
- 12: **end for**
- 13: **return**  $M_K^s$

---

**Base Model** For a quick validation, we further revise a recent REC model called SimREC (Luo et al. 2022) as our base model. As shown in Fig. 2, given the input image and

text, the visual backbone and the text encoder extract features of two modalities, upon which the multi-modal fusion branch is used to conduct multi-modal interactions. Finally, the decoder is applied to predict the mask of the referent.

## Experiments

### Datasets and Metrics

**RefCOCO, RefCOCO+ and RefCOCOg** are three widely-used RES benchmark datasets (Yu et al. 2016; Mao et al. 2015; Nagaraja, Morariu, and Davis 2016). In particular, RefCOCO and RefCOCO+ contain 140k natural language expressions for 50k objects in 20k images. The descriptions of RefCOCO are mainly about spatial content, whereas RefCOCO+ has a greater prevalence of attribute and relative spatial descriptions. In RefCOCO and RefCOCO+, their splits *testA* and *testB* are about people and objects, respectively. RefCOCOg has a comparable dataset size to RefCOCO and RefCOCO+, *i.e.*, 104k expressions for 54k objects in 26k image, but its descriptions are more complex. RefCOCOg has two different partitions, *i.e.*, google (Nagaraja, Morariu, and Davis 2016) and UMD partitions (Mao et al. 2015). In this paper, we use UMD partition for comparison.

**Visual Genome** (Krishna et al. 2016) is a large-scale vision-language dataset, containing 108,077 images taken from the MSCOCO dataset, 1.7M vqa examples, 5.4M region descriptions, 3.8M object instances, 2.8M attributes, 2.3M visual relationships. Here, the region descriptions and corresponding boxes can be used as the omni-labels.

**Metrics.** Following the settings of (Yang et al. 2021b; Liu, Ding, and Jiang 2023; Liu et al. 2023), We use overall *intersection-over-union (IoU)*, *mean intersection-over-union (mIoU)*, and *precision* as the evaluation metrics for our experiments.

### Implementation Details

The model configurations, such as visual backbone, are kept the same with previous works (Luo et al. 2022). Adam is used as the optimizer with a learning rate of  $1e-4$ , and a batch size of 64. In Omni-RES, EMA (Tarvainen and Valpola 2017) coefficient is set to 0.9996 for updating the Teacher model. By default, the thresholds applied for filtering the teacher’s prediction are set between 0.7 and 0.2, and  $\gamma$  are set to 0.2. For omni-training with boxes and points, the threshold is adjusted between 0.5 and 0.2, and the weight of omni-loss is set to 1. More details can refer to our source code.

### Quantitative Analysis

**Ablation Study.** We first ablate Omni-RES with different types of omni-labels and compare it with *the semi- and fully supervised baseline* in Tab. 1. Omni-None also refers to the semi-supervised baseline. From this table, we first observe that the semi-supervised baseline (Omni-None) can already outperform fully supervised baseline by a large margin, *e.g.*, +9.52% on 1% RefCOCO. With the help of our omni-training, *e.g.*, Omni-Point and Omni-Box, the performance boost significantly, *e.g.*, +24.47 by Omni-Box on RefCOCO *testA*. However, we also see that the performance of

Omni-Point varies greatly under different splits of labeled data. With 10% labeled data, its performance is close to Omni-Box, while the gap becomes larger when the label information is less, *e.g.*, 1%. To explain, when the label information is very limited, the quality of pseudo-masks are too poor to meet the referring point, *e.g.*, very scattered segmentation results. This case also reflects the challenge of RES towards omni-supervised learning and the inferior pseudo-label quality than other tasks.

In Tab. 2, we compare the proposed *Active Pseudo-Label Refinement (APLR)* with a set of alternative filtering schemes. In particular,  $APLR_{point}$  and  $APLR_{w/ofiltering}$  denote the used metric in Eq. 6 and the the removal of filtering strategy, respectively. Point distance and  $APLR_{box}$  denote the filtering metric defined by geometry distance and the metric defined in Eq. 7, respectively. Compared with it, *box filtering* only suppress the pixels outside the box. *Average confidence* means the average positive pixel confidence within the omni-box. From Tab. 2, we can see that the alternative filtering strategies can improve the omni-RES performance to some extent. However, their benefits are very marginal. Meanwhile, it is also not very significant to directly apply the filtering strategy from other Omni-methods (Wang et al. 2022), *i.e.* point distance. The proposed APLR for omni-point and omni-box show obvious advantages to the alternative methods, especially for  $APLR_{w/ofiltering}$  and *box filtering*. These results on one hand confirm the effectiveness of APLR for Omni-RES, and on the other hand suggest that the significance of pseudo-label quality.

**Generalization to LAVT and ReLA.** To examine the generalization ability of Omni-RES, we further apply it to two advanced RES models, namely LAVT (Yang et al. 2021b) and ReLA (Liu, Ding, and Jiang 2023), of which results are given in Tab. 3. In particular, LAVT and ReLA demonstrate strong supervised performance on 10% RefCOCO. Even so, we can still observe the significant gains of Omni-RES on these methods. For instance, the relative performance improvements of Omni-Point and Omni-Box can be up to +5.80% and +9.15% on RefCOCO+ *testB*, respectively. For ReLA, the improvements are more significant, *e.g.*, +8.19% and +9.88%. These results well confirm that Omni-RES can collaborate well with existing SOTA RES models, and further improve their performance.

**Comparison with the State-of-the-art.** In Tab. 4, we compare SimRES and ReLA trained by Omni-Box with the existing RES approaches. In particular, we conduct the training of Omni-Box with the labeled data of three RefCOCO-series datasets and the weakly labeled data of Visual Genome (Krishna et al. 2016)<sup>1</sup>. From this table, the first observation is that Omni-Box obviously outperform its fully supervised counterpart, *e.g.*, +7.22% on RefCOCOg *test*. With the help of Omni-Box,  $ReLA_{omni}$  can achieve new SOTA performances on three RES datasets, *e.g.*, 80.66% on RefCOCO *testA*. When compared to the existing SOTA model, *i.e.*, PolyFormer (Liu et al. 2023), the performance

<sup>1</sup>the images in the validation and test splits of three benchmarks are removed.

Table 1: Ablation study of Omni-RES with different types of omni-labels. Here, Omni-None means that the unlabeled data are used, which can be regarded as the semi-supervise baseline.

Method	Percentage	RefCOCO			RefCOCO+			RefCOCOg	
		val	testA	testB	val	testA	testB	val	test
Fully Supervised	1%	32.07	34.79	27.61	19.45	21.60	15.11	24.53	24.05
Omni-None	1%	41.01	44.31	37.55	23.46	24.03	20.27	29.69	29.38
Omni-Point	1%	47.59	50.04	45.55	33.18	36.47	29.47	35.24	37.11
Omni-Box	1%	55.94	59.26	53.04	41.12	42.99	35.88	43.83	46.18
Fully Supervised	5%	42.75	45.26	41.53	28.18	29.01	24.71	32.73	34.13
Omni-None	5%	53.26	55.82	50.70	36.55	38.96	31.21	39.68	39.25
Omni-Point	5%	57.10	60.59	55.10	42.76	46.72	36.95	45.29	45.24
Omni-Box	5%	60.07	62.89	58.22	46.78	49.09	38.83	48.61	49.00
Fully Supervised	10%	47.78	48.62	45.58	31.69	32.47	27.84	38.39	37.57
Omni-None	10%	57.19	60.04	53.97	41.48	43.41	36.22	43.90	43.44
Omni-Point	10%	60.94	64.02	58.60	45.89	48.36	39.09	47.08	46.74
Omni-Box	10%	62.55	64.74	58.76	47.85	50.04	41.61	49.41	49.08

Table 2: Comparison of the proposed Active Pseudo-Label Refinement (APLR) with alternative pseudo-label filtering schemes. The proportion of fully labeled data is 1%.

Method	RefCOCO			RefCOCO+			RefCOCOg	
	val	testA	testB	val	testA	testB	val	test
None	41.01	44.31	37.55	23.46	24.03	20.27	29.69	29.38
point distance	40.90	44.24	36.90	26.29	28.04	21.38	29.09	29.42
$APLR_w/ofiltering$	43.81	47.05	38.64	25.44	24.80	19.54	31.40	31.09
$APLR_{point}$	47.59	50.04	45.55	33.18	36.47	29.47	35.24	37.11
Average confidence	51.33	56.05	46.63	30.88	32.21	25.33	36.69	36.61
Box Filtering	50.28	54.43	45.76	30.50	31.08	25.32	34.14	33.72
$APLR_{box}$	55.94	59.26	53.04	41.12	42.99	35.88	43.83	46.18

Table 3: Generalizations of Omni-RES to the state-of-the-art RES models, *i.e.*, LAVT (Yang et al. 2021b) and ReLA (Liu, Ding, and Jiang 2023). Omni-P and Omni-B denotes the use of points and boxes as the omni-labels, respectively. The proportion of fully labeled data is 10%.

Method	Model	RefCOCO			RefCOCO+		
		val	testA	testB	val	testA	testB
Supervise	LAVT	57.25	61.63	52.70	44.24	49.79	37.04
Omni-P	LAVT	64.70	68.93	60.27	50.67	56.73	42.84
Omni-B	LAVT	66.00	68.96	62.08	53.31	59.12	46.19
Supervise	ReLA	60.11	63.12	55.25	45.10	51.97	36.84
Omni-P	ReLA	67.29	70.34	62.89	54.19	61.20	45.03
Omni-B	ReLA	68.71	72.08	65.28	55.86	62.17	46.72

gains of  $ReLA_{omni}$  become significant on the more challenging datasets, such as RefCOCO+ *testB*, and RefCOCOg *test*. These results also suggest that our Omni-training can facilitate the learning of these difficult examples. Overall, these results further confirm the effectiveness of Omni-RES,

and also validate our motivation about the use of weakly labeled data.

### Qualitative Analysis

To obtain deep insights into Omni-RES, we further visualize their results of pseudo-label refinements in Fig. 3, which shows the pseudo-masks with and without the proposed APRL. We can first observe that the qualities of original pseudo-labels are poor, which often fails to completely mask the referent or has incorrect predictions. For instance, the model segment several parts of two people in the 3-th example. With APRL, *i.e.*, Point and Box, their qualities are greatly improved. In terms of APRL with the omni-labels of points, the segmentations for the incorrect targets can be well handled, *e.g.*, the 2-th examples, suggesting its merits in locating referents. However, its refinement to the mask contour is still insufficient. For example, it still includes the background to the referent of bear in the 1-st example. In contrast, APRL with grounding boxes can filter out all incorrect mask pixels outside the box, leading to better masks in details. Meanwhile, its ability of spatial grounding is also as well as the points. Overall, these results further confirm the merits of Omni-RES.

Table 4: Comparison with the State-of-the-art methods on three RES datasets. RefCOCO, RefCOCO+ and RefCOCOg are used as the labeled data, and VG is used as the omni-labeled data.

Method	Visual Backbone	Textual Encoder	RefCOCO			RefCOCO+			RefCOCOg	
			val	testA	testB	val	testA	testB	val	test
MAttNet (Yu et al. 2018)	MaskRCNN-R101	bi-LSTM	56.51	62.37	51.70	46.67	52.39	40.08	47.64	48.61
CMSA (Ye et al. 2019)	DeepLab-R101	None	58.32	60.61	55.09	43.76	47.60	37.89	-	-
CAC (Chen et al. 2019b)	ResNet101	bi-LSTM	58.90	61.77	53.81	-	-	-	46.37	46.95
STEP (Chen et al. 2019a)	DeepLab-R101	bi-LSTM	60.04	63.46	57.97	48.19	52.33	40.41	-	-
BRINet (Hu et al. 2020)	DeepLab-R101	LSTM	60.98	62.99	59.21	48.17	52.32	42.11	-	-
CMPC (Huang et al. 2020)	DeepLab-R101	LSTM	61.36	64.53	59.64	49.56	53.44	43.23	-	-
LSCM (Hui et al. 2020)	DeepLab-R101	LSTM	61.47	64.99	59.55	49.34	53.12	43.50	-	-
CMPC+ (Liu et al. 2021a)	DeepLab-R101	LSTM	62.47	65.08	60.82	50.25	54.04	43.47	-	-
MCN (Luo et al. 2020b)	Darknet53	bi-GRU	62.44	64.20	59.71	50.62	54.99	44.69	49.22	49.40
EFN (Feng et al. 2021)	ResNet101	bi-GRU	62.76	65.69	59.67	51.50	55.24	43.01	-	-
BUSNet (Yang et al. 2021a)	DeepLab-R101	Self-Att	63.27	66.41	61.39	51.76	56.87	44.13	-	-
CGAN (Luo et al. 2020a)	DeepLab-R101	bi-GRU	64.86	68.04	62.07	51.03	55.51	44.06	51.01	51.69
ISFP (Liu, Jiang, and Ding 2022)	Darknet53	bi-GRU	65.19	68.45	62.73	52.70	56.77	46.39	52.67	53.00
LTS (Jing et al. 2021)	Darknet53	bi-GRU	65.43	67.76	63.08	54.21	58.32	48.02	54.40	54.25
ReSTR (Kim et al. 2022)	ViT-B	Transformer	67.22	69.30	64.45	55.78	60.44	48.27	-	-
MaIL (Li et al. 2021c)	ViLT	BERT	70.13	71.71	66.92	62.23	65.92	56.06	62.45	62.87
CRIS (Wang et al. 2021)	CLIP-R101	CLIP	70.47	73.18	66.10	62.27	68.08	53.68	59.87	60.36
LAVT (Yang et al. 2021b)	Swin-B	BERT	72.73	75.82	68.79	62.14	68.38	55.10	61.24	62.09
VLT (Ding et al. 2022)	Swin-B	BERT	72.96	75.96	69.60	63.53	68.43	56.92	63.49	66.22
ReLA (Liu, Ding, and Jiang 2023)	Swin-B	BERT	73.82	76.48	70.18	66.04	71.02	57.65	65.00	65.97
PolyFormer (Liu et al. 2023)	Swin-L	BERT	75.96	78.29	73.25	69.33	74.56	61.87	69.20	70.19
<i>SimRES<sub>omni</sub></i> (Ours)	Darknet53	bi-GRU	68.58	70.54	63.10	57.02	59.42	48.53	59.56	59.71
<i>ReLA<sub>omni</sub></i> (Ours)	Swin-B	BERT	<b>78.69</b>	<b>80.66</b>	<b>75.53</b>	<b>71.06</b>	<b>74.60</b>	<b>63.72</b>	<b>71.40</b>	<b>73.19</b>

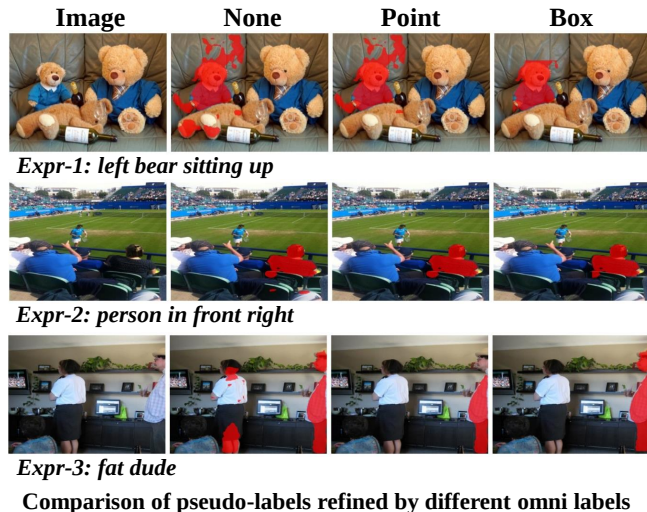


Figure 3: Visualizations of Omni-RES. Without any refinements, the pseudo-masks are often scattered and erroneous, while Omni-RES can use the proposed Active Pseudo-Label Refinement to improve the quality of pseudo-masks based on omni-labels of points or boxes.

## Conclusions

In this paper, we focus on the issue of expensive instance-level annotation and insufficient label information of RES, and propose a novel omni-supervised learning task, termed Omni-RES. Omni-RES aims to make full use of unlabeled, fully-labeled and weak labels to facilitate efficient RES training, *i.e.*, the grounding boxes and referring points. To accomplish this task, we also propose a strong baseline method based on the recently popular teacher-student framework. In this method, the omni-labels, *i.e.*, such as referring points and grounding boxes are not directly transformed into supervision signals for RES training. Instead, we use them as reference to produce high-quality pseudo-masks for teacher-student learning. To validate Omni-RES, we apply it a simple base model called SimRES and conduct extensive experiments on three RES benchmarks. The experimental results show the great advantages of Omni-RES than the supervised and semi-supervised baselines. Notably, with only 10% fully labeled data, Omni-RES can achieve the 100% supervised performance, strongly confirming the benefits of Omni-RES. In addition, the generalization of Omni-RES is also validated on recently proposed RES models called LAVT and ReLA. Finally, we achieve the SOTA result using ReLA model with extra Omni-Box labels, which obviously outperforms the existing SOTA model called PolyFormer.

## Acknowledgements

This work was supported by National Key R&D Program of China (No.2022ZD0118201), the National Science Fund for Distinguished Young Scholars (No.62025603), the National Natural Science Foundation of China (No.U21B2037, No.U22B2051, No.62176222, No.62176223, No.62176226, No.62072386, No.62072387, No.62072389, No.62002305 and No.62272401), and the Natural Science Foundation of Fujian Province of China (No.2021J01002, No.2022J06001), and the China Fundamental Research Funds for the Central Universities (Grant No.20720220068).

## References

- Ahn, J.; and Kwak, S. 2018a. Learning Pixel-level Semantic Affinity with Image-level Supervision for Weakly Supervised Semantic Segmentation.
- Ahn, J.; and Kwak, S. 2018b. Learning Pixel-level Semantic Affinity with Image-level Supervision for Weakly Supervised Semantic Segmentation.
- Carion, N.; Massa, F.; Synnaeve, G.; Usunier, N.; Kirillov, A.; and Zagoruyko, S. 2020. End-to-End Object Detection with Transformers.
- Chen, D.-J.; Jia, S.; Lo, Y.-C.; Chen, H.-T.; and Liu, T.-L. 2019a. See-Through-Text Grouping for Referring Image Segmentation. In *2019 IEEE/CVF International Conference on Computer Vision (ICCV)*, 7453–7462.
- Chen, H.; Sun, K.; Tian, Z.; Shen, C.; Huang, Y.; and Yan, Y. 2020. BlendMask: Top-Down Meets Bottom-Up for Instance Segmentation.
- Chen, L.-C.; Papandreou, G.; Kokkinos, I.; Murphy, K.; and Yuille, A. L. 2016. DeepLab: Semantic Image Segmentation with Deep Convolutional Nets, Atrous Convolution, and Fully Connected CRFs.
- Chen, Y.-W.; Tsai, Y.-H.; Wang, T.; Lin, Y.-Y.; and Yang, M.-H. 2019b. Referring Expression Object Segmentation with Caption-Aware Consistency.
- Ding, H.; Liu, C.; Wang, S.; and Jiang, X. 2022. VLT: Vision-Language Transformer and Query Generation for Referring Segmentation. *IEEE Transactions on Pattern Analysis and Machine Intelligence*, 1–16.
- Feng, G.; Hu, Z.; Zhang, L.; and Lu, H. 2021. Encoder Fusion Network with Co-Attention Embedding for Referring Image Segmentation.
- Feng, G.; Zhang, L.; Hu, Z.; and Lu, H. 2022. Learning From Box Annotations for Referring Image Segmentation. *IEEE Transactions on Neural Networks and Learning Systems*, 1–11.
- He, K.; Gkioxari, G.; Dollár, P.; and Girshick, R. 2017. Mask R-CNN.
- Hu, R.; Rohrbach, M.; and Darrell, T. 2016. Segmentation from Natural Language Expressions.
- Hu, Z.; Feng, G.; Sun, J.; Zhang, L.; and Lu, H. 2020. Bi-Directional Relationship Inferring Network for Referring Image Segmentation. In *2020 IEEE/CVF Conference on Computer Vision and Pattern Recognition (CVPR)*, 4423–4432.
- Huang, S.; Hui, T.; Liu, S.; Li, G.; Wei, Y.; Han, J.; Liu, L.; and Li, B. 2020. Referring Image Segmentation via Cross-Modal Progressive Comprehension.
- Hui, T.; Liu, S.; Huang, S.; Li, G.; Yu, S.; Zhang, F.; and Han, J. 2020. Linguistic Structure Guided Context Modeling for Referring Image Segmentation.
- Jiang, P.-T.; Han, L.-H.; Hou, Q.; Cheng, M.-M.; and Wei, Y. 2022. Online Attention Accumulation for Weakly Supervised Semantic Segmentation. *IEEE Transactions on Pattern Analysis and Machine Intelligence*, 44(10): 7062–7077.
- Jing, Y.; Kong, T.; Wang, W.; Wang, L.; Li, L.; and Tan, T. 2021. Locate then Segment: A Strong Pipeline for Referring Image Segmentation.
- Kim, N.; Kim, D.; Lan, C.; Zeng, W.; and Kwak, S. 2022. ReSTR: Convolution-free Referring Image Segmentation Using Transformers.
- Kirillov, A.; He, K.; Girshick, R.; Rother, C.; and Dollár, P. 2018. Panoptic Segmentation.
- Krishna, R.; Zhu, Y.; Groth, O.; Johnson, J.; Hata, K.; Kravitz, J.; Chen, S.; Kalantidis, Y.; Li, L.-J.; Shamma, D. A.; Bernstein, M. S.; and Li, F.-F. 2016. Visual Genome: Connecting Language and Vision Using Crowdsourced Dense Image Annotations.
- Li, H.; Sun, M.; Xiao, J.; Lim, E. G.; and Zhao, Y. 2022. Fully and Weakly Supervised Referring Expression Segmentation with End-to-End Learning.
- Li, H.; Wu, Z.; Shrivastava, A.; and Davis, L. S. 2021a. Rethinking Pseudo Labels for Semi-Supervised Object Detection.
- Li, H.; Wu, Z.; Shrivastava, A.; and Davis, L. S. 2021b. Rethinking Pseudo Labels for Semi-Supervised Object Detection.
- Li, M.; and Sigal, L. 2021. Referring Transformer: A One-step Approach to Multi-task Visual Grounding.
- Li, Q.; Arnab, A.; and Torr, P. H. S. 2018. Weakly- and Semi-Supervised Panoptic Segmentation.
- Li, R.; Li, K.; Kuo, Y.-C.; Shu, M.; Qi, X.; Shen, X.; and Jia, J. 2018. Referring Image Segmentation via Recurrent Refinement Networks. In *2018 IEEE/CVF Conference on Computer Vision and Pattern Recognition*, 5745–5753.
- Li, Z.; Wang, M.; Mei, J.; and Liu, Y. 2021c. MaIL: A Unified Mask-Image-Language Trimodal Network for Referring Image Segmentation.
- Lin, T.-Y.; Maire, M.; Belongie, S.; Bourdev, L.; Girshick, R.; Hays, J.; Perona, P.; Ramanan, D.; Zitnick, C. L.; and Dollár, P. 2014. Microsoft COCO: Common Objects in Context.
- Liu, C.; Ding, H.; and Jiang, X. 2023. GRES: Generalized Referring Expression Segmentation. arXiv:2306.00968.
- Liu, C.; Jiang, X.; and Ding, H. 2022. Instance-Specific Feature Propagation for Referring Segmentation. *IEEE Transactions on Multimedia*, 1–1.
- Liu, C.; Lin, Z.; Shen, X.; Yang, J.; Lu, X.; and Yuille, A. 2017. Recurrent Multimodal Interaction for Referring Image Segmentation.



- Liu, D.; Zhang, H.; Wu, F.; and Zha, Z.-J. 2018. Learning to Assemble Neural Module Tree Networks for Visual Grounding.
- Liu, J.; Ding, H.; Cai, Z.; Zhang, Y.; Satzoda, R. K.; Mahadevan, V.; and Manmatha, R. 2023. PolyFormer: Referring Image Segmentation as Sequential Polygon Generation. arXiv:2302.07387.
- Liu, S.; Hui, T.; Huang, S.; Wei, Y.; Li, B.; and Li, G. 2021a. Cross-Modal Progressive Comprehension for Referring Segmentation.
- Liu, Y.-C.; Ma, C.-Y.; He, Z.; Kuo, C.-W.; Chen, K.; Zhang, P.; Wu, B.; Kira, Z.; and Vajda, P. 2021b. Unbiased Teacher for Semi-Supervised Object Detection.
- Long, J.; Shelhamer, E.; and Darrell, T. 2014. Fully Convolutional Networks for Semantic Segmentation.
- Luo, G.; Zhou, Y.; Ji, R.; Sun, X.; Su, J.; Lin, C.-W.; and Tian, Q. 2020a. Cascade Grouped Attention Network for Referring Expression Segmentation. In *Proceedings of the 28th ACM International Conference on Multimedia, MM '20*, 1274–1282. New York, NY, USA: Association for Computing Machinery. ISBN 9781450379885.
- Luo, G.; Zhou, Y.; Ren, T.; Chen, S.; Sun, X.; and Ji, R. 2023a. Cheap and Quick: Efficient Vision-Language Instruction Tuning for Large Language Models. arXiv:2305.15023.
- Luo, G.; Zhou, Y.; Sun, J.; Huang, S.; Sun, X.; Ye, Q.; Wu, Y.; and Ji, R. 2022. What Goes beyond Multi-modal Fusion in One-stage Referring Expression Comprehension: An Empirical Study.
- Luo, G.; Zhou, Y.; Sun, X.; Cao, L.; Wu, C.; Deng, C.; and Ji, R. 2020b. Multi-task Collaborative Network for Joint Referring Expression Comprehension and Segmentation.
- Luo, G.; Zhou, Y.; Sun, X.; Wu, Y.; Gao, Y.; and Ji, R. 2023b. Towards Language-guided Visual Recognition via Dynamic Convolutions. arXiv:2110.08797.
- Mao, J.; Huang, J.; Toshev, A.; Camburu, O.; Yuille, A.; and Murphy, K. 2015. Generation and Comprehension of Unambiguous Object Descriptions.
- Margffoy-Tuay, E.; Pérez, J. C.; Botero, E.; and Arbeláez, P. 2018. Dynamic Multimodal Instance Segmentation guided by natural language queries.
- Mi, P.; Lin, J.; Zhou, Y.; Shen, Y.; Luo, G.; Sun, X.; Cao, L.; Fu, R.; Xu, Q.; and Ji, R. 2022. Active Teacher for Semi-Supervised Object Detection. In *2022 IEEE/CVF Conference on Computer Vision and Pattern Recognition (CVPR)*, 14462–14471.
- Nagaraja, V. K.; Morariu, V. I.; and Davis, L. S. 2016. Modeling Context Between Objects for Referring Expression Understanding.
- Oh, Y.; Kim, B.; and Ham, B. 2021. Background-Aware Pooling and Noise-Aware Loss for Weakly-Supervised Semantic Segmentation.
- Ordonez, V.; Kulkarni, G.; and Berg, T. 2011. Im2Text: Describing Images Using 1 Million Captioned Photographs. In Shawe-Taylor, J.; Zemel, R.; Bartlett, P.; Pereira, F.; and Weinberger, K., eds., *Advances in Neural Information Processing Systems*, volume 24. Curran Associates, Inc.
- Radosavovic, I.; Dollár, P.; Girshick, R.; Gkioxari, G.; and He, K. 2017. Data Distillation: Towards Omni-Supervised Learning.
- Ren, Z.; Yu, Z.; Yang, X.; Liu, M.-Y.; Schwing, A. G.; and Kautz, J. 2020. UFO<sup>2</sup>: A Unified Framework towards Omni-supervised Object Detection.
- Sharma, P.; Ding, N.; Goodman, S.; and Soricut, R. 2018. Conceptual Captions: A Cleaned, Hypernymed, Image Alt-text Dataset For Automatic Image Captioning. In *Proceedings of the 56th Annual Meeting of the Association for Computational Linguistics (Volume 1: Long Papers)*, 2556–2565. Melbourne, Australia: Association for Computational Linguistics.
- Sohn, K.; Zhang, Z.; Li, C.-L.; Zhang, H.; Lee, C.-Y.; and Pfister, T. 2020. A Simple Semi-Supervised Learning Framework for Object Detection.
- Strudel, R.; Laptev, I.; and Schmid, C. 2022. Weakly-supervised segmentation of referring expressions.
- Sun, G.; Wang, W.; Dai, J.; and Van Gool, L. 2020. Mining Cross-Image Semantics for Weakly Supervised Semantic Segmentation.
- Suzuki, S.; et al. 1985. Topological structural analysis of digitized binary images by border following. *Computer vision, graphics, and image processing*, 30(1): 32–46.
- Tang, Y.; Chen, W.; Luo, Y.; and Zhang, Y. 2021. Humble Teachers Teach Better Students for Semi-Supervised Object Detection.
- Tarvainen, A.; and Valpola, H. 2017. Mean teachers are better role models: Weight-averaged consistency targets improve semi-supervised deep learning results.
- Wang, P.; Cai, Z.; Yang, H.; Swaminathan, G.; Vasconcelos, N.; Schiele, B.; and Soatto, S. 2022. Omni-DETR: Omni-Supervised Object Detection with Transformers.
- Wang, Y.; Zhang, J.; Kan, M.; Shan, S.; and Chen, X. 2020a. Self-supervised Equivariant Attention Mechanism for Weakly Supervised Semantic Segmentation.
- Wang, Y.; Zhang, J.; Kan, M.; Shan, S.; and Chen, X. 2020b. Self-supervised Equivariant Attention Mechanism for Weakly Supervised Semantic Segmentation.
- Wang, Z.; Lu, Y.; Li, Q.; Tao, X.; Guo, Y.; Gong, M.; and Liu, T. 2021. CRIS: CLIP-Driven Referring Image Segmentation.
- Xu, M.; Zhang, Z.; Hu, H.; Wang, J.; Wang, L.; Wei, F.; Bai, X.; and Liu, Z. 2021. End-to-End Semi-Supervised Object Detection with Soft Teacher.
- Yang, S.; Xia, M.; Li, G.; Zhou, H.-Y.; and Yu, Y. 2021a. Bottom-Up Shift and Reasoning for Referring Image Segmentation. In *2021 IEEE/CVF Conference on Computer Vision and Pattern Recognition (CVPR)*, 11261–11270.
- Yang, Z.; Wang, J.; Tang, Y.; Chen, K.; Zhao, H.; and Torr, P. H. S. 2021b. LAVT: Language-Aware Vision Transformer for Referring Image Segmentation.

- Ye, L.; Rochan, M.; Liu, Z.; and Wang, Y. 2019. Cross-Modal Self-Attention Network for Referring Image Segmentation.
- Yu, L.; Lin, Z.; Shen, X.; Yang, J.; Lu, X.; Bansal, M.; and Berg, T. L. 2018. MAttNet: Modular Attention Network for Referring Expression Comprehension.
- Yu, L.; Poirson, P.; Yang, S.; Berg, A. C.; and Berg, T. L. 2016. Modeling Context in Referring Expressions.
- Zhang, D.; Zhang, H.; Tang, J.; Hua, X.; and Sun, Q. 2020. Causal Intervention for Weakly-Supervised Semantic Segmentation.
- Zhao, W.; Rao, Y.; Liu, Z.; Liu, B.; Zhou, J.; and Lu, J. 2023. Unleashing Text-to-Image Diffusion Models for Visual Perception. arXiv:2303.02153.
- Zhou, B.; Khosla, A.; Lapedriza, A.; Oliva, A.; and Torralba, A. 2015. Learning Deep Features for Discriminative Localization.
- Zhu, C.; Zhou, Y.; Shen, Y.; Luo, G.; Pan, X.; Lin, M.; Chen, C.; Cao, L.; Sun, X.; and Ji, R. 2022. SeqTR: A Simple Yet Universal Network for Visual Grounding. In *Lecture Notes in Computer Science*, 598–615. Springer Nature Switzerland.